

**Spectral Moment Analysis of the Deuterium-Deuterium Neutron Energy  
Distribution from Inertial Confinement Fusion on OMEGA**

A. DeVault

Penfield High School

Advisors: C. J. Forrest, O. Mannion

*Laboratory for Laser Energetics, University of Rochester, 250 East River Road*

*Rochester, New York 14623-1299, USA*

December 2019

## ABSTRACT

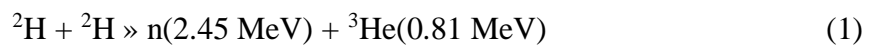
Nuclear diagnostics are essential for inferring the conditions of the deuterium-deuterium (DD) fuel during compression for inertial confinement fusion experiments. The plasma temperature and velocity influence the neutron energy distribution emitted from the fusing target. Bulk flow of the plasma affects the first spectral moment (mean) while the ion temperature affects the second spectral moment (variance). These signatures indicate the presence of fluid motion during hot-spot formation as well as the temperature of the plasma, both of which are important metrics to assess implosion performance. A forward-fit analysis technique was developed to obtain the ion temperature and bulk flow velocity from a primary (DD) neutron energy distribution obtained from a neutron time-of-flight spectrometer. This approach was utilized in a recent campaign to measure the effect of low-mode nonuniformities induced through intentional target offsets. The technique was tested using existing data and simulations and was found to be relatively accurate in determining ion temperatures and bulk flow velocities. A positive, linear relationship was found to exist between offset and bulk flow velocity. A low-mode asymmetry introduced by a systematic offset/imbalance in the laser-target system can be mitigated using a standardized offset based on this relationship.

## I. INTRODUCTION

Studying inertial confinement fusion (ICF) is a primary objective at the Laboratory for Laser Energetics (LLE). ICF targets are made out of a thin spherical ablator shell less than 1 millimeter in diameter with both solid and gaseous fuel within.

The energy deposition required to trigger nuclear fusion is achieved through the use of high-power UV lasers. The 60 OMEGA UV laser beams deliver up to 30 kJ of energy onto the ICF target during a nominal 1-ns square pulse. The symmetric illumination rapidly heats and ablates the thin shell. Following Newton's third law, every action has an equal and opposite reaction, and thus the force exerted by the ablating shell provides an inward compressive force upon the target, which, in this work, is filled with deuterium–deuterium (DD) fuel. In an ideal, symmetric implosion, all kinetic energy from the ablator would be transferred to ion thermal energy, heating the very center of the imploding target (the hot spot) to reach the extreme temperature and pressure conditions required to initiate fusion. Temperatures of approximately 100 million Kelvin and pressures exceeding 200 billion atm must be reached in order to overcome the repulsive Coulomb force between two light nuclei and trigger fusion. However, in a realistic implosion, imperfections and asymmetries lead to imperfect translation of kinetic energy to thermal energy, leading to residual kinetic energy in the system, which manifests as flow velocities during the formation of the hot spot.

Bulk flow velocity is characterized as the net velocity of the fusing plasma. Flow velocities are a symptom of asymmetrical implosions, typically caused by unbalanced energy deposition. In order to detect bulk flow velocities, the spectra of energetic neutrons emitted by the fusing plasma can be analyzed. Equation 1 illustrates the relevant neutron-producing fusion reaction of deuterium-deuterium, along with the approximate energies of the products.



The neutron spectra can be detected by a neutron time-of-flight (nTOF) spectrometer, which relies on a scintillator and photomultiplier tube to relay a signal relative to the number of neutrons incident on the detector. If the time of the implosion is known relative to the neutron detection signal, and the detector is at a known distance from the target, then the velocity and therefore energy of the neutrons can be determined. Since deuterium-deuterium fusion is known to emit approximately monoenergetic neutrons, any deviation from this mean energy can be treated as a Doppler shift in order to determine the velocity of the fusing plasma towards or away from the detector. While bulk flow contributes to shifts in mean energy, ion temperature ( $T_{\text{ion}}$ ) affects the mean energy to a small degree [1], but mainly influences the broadening of the spectra. Since the neutron spectrum for deuterium-deuterium fusion can be fit using a modified gaussian, its mean energy and broadening (which are used to determine bulk flow velocity and  $T_{\text{ion}}$ , respectively) can be described as spectral moments, with the first spectral moment being the mean, and the second spectral moment being the variance (broadening).

In order to measure the effect of asymmetries on an ICF target, campaigns have been held utilizing intentional target offsets to induce low modes of nonuniformity. Offsetting the target will shift the focus of the laser power away from the center of the target but will not alter the laser power balance relative to the focus of the beams. Experiments designed with induced modes and asymmetries help scientists to better understand asymmetries in the laser-target system that may be preventing ideal implosions. Induced modes can potentially serve as a tool for correcting any inherent

asymmetries in the laser, as these induced modes can be used to counteract unbalanced energy deposition.

An analysis technique was developed in order to explore the effect that these induced modes have on the bulk flow, yield, and ion temperature of deuterium-deuterium fusion experiments. Utilizing data retrieved by neutron time-of-flight spectrometers, a neutron energy distribution was modeled and subsequently used to determine the spectral moments of the data. Using this analysis, dozens of nominal shots were analyzed to identify correlations between known variables such as shell thickness, and ion temperature or bulk flow velocity. The technique was also used on campaign shots to determine the relationship between target offset and the bulk flow velocity of the fusing plasma (an indicator of the symmetry of the implosion).

## **II. FUSION NEUTRON SPECTRA**

DD fusion's single, approximately monoenergetic, gaussian neutron distribution allows for accurate curve fitting and analysis. In DD fusion, two hydrogen isotopes combine to form Helium-4 before instantly decaying into Helium-3 and a 2.45 MeV neutron (Equation 1). In a perfectly symmetric implosion under ideal conditions, a neutron distribution as pictured in Figure 2.1(a) would be expected. However, when asymmetries are induced, the presence of bulk flow velocity will alter the energy distribution (as pictured in Figure 2.1(b) ). As a bulk flow velocity away from the detector is observed, lower mean energies will be interpreted (as represented by the

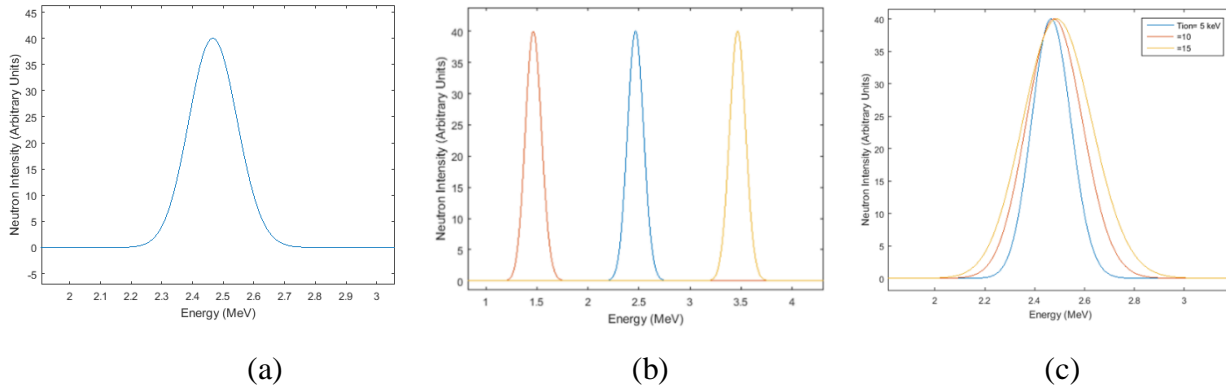


Figure 2.1(a): The neutron energy distribution expected from a symmetrical implosion.  
 (b): A highly exaggerated display of the effect that a bulk flow velocity will have on a gaussian neutron distribution.  
 (c): A display of the broadening and slight shifting of the neutron energy distribution as the ion temperature increases from 5 to 15 keV

orange curve), while velocities towards the detector will result in higher measured mean energies (as represented by the yellow curve). As  $T_{\text{ion}}$  increases (Figure 2.1(c)), the mean energy will shift slightly towards higher energies, and broadening will increase. The simulated effect of variable bulk flow velocity and ion temperature shown in Figures 2.1(a)-2.1(c) can be used to deduce the mean ion temperature and bulk flow velocity of experimental implosions. The effects of bulk motion and ion temperature on neutron distribution used here are consistent with those identified by Munro at the National Ignition Facility [2].

By utilizing induced modes through target offset, a bulk flow velocity of 0 can be pursued, indicating a more symmetric implosion along the line of sight of the detector, minimizing the residual kinetic energy present and improving the implosion efficiency.

### III. EXPERIMENTAL DETAILS

In terms of detecting asymmetries, the most insightful diagnostic is the neutron time-of-flight (nTOF) signal. Figure 3.1 shows the location of an nTOF detector on OMEGA and a schematic of its key components. Using a scintillator and a photomultiplier tube (PMT), the number of neutrons incident upon the scintillator can be measured as a function of time, allowing for the deduction of the neutron velocity spectrum and therefore the energy spectrum. The neutron energy distribution ( $dN/dE$ ) determined by the nTOF signal can be used to determine the approximate ion temperature of the fusing plasma and the bulk flow velocity of the target.

Figure 3.1 shows that there is a clear line of sight from the fusing target to the nTOF detector, 13.4 m away. The xylene scintillator luminesces when struck by neutrons, allowing for a conversion of neutrons to photons. The photon signal is strengthened by a PMT and then digitized using an oscilloscope. While the analysis performed was based on the measurements and specifications of LLE's facilities, it may be easily altered to fit the specifications of other laboratories.

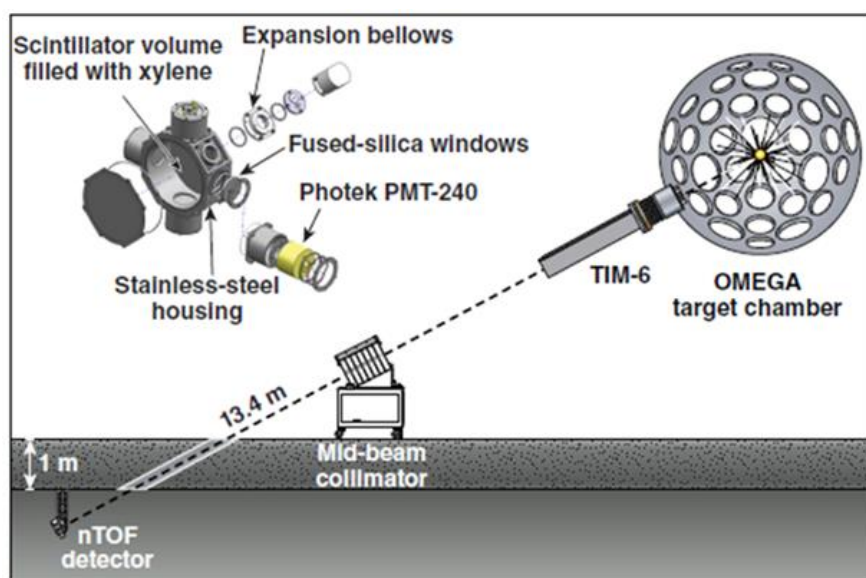


Figure 3.1  
Location of a nTOF detector on OMEGA. It uses a xylene scintillator at a distance of 13.4 m from the site of fusion

As nTOF diagnostics and the deduction of neutron energy spectra rely entirely on the measurement of the time it takes for neutrons to reach a scintillator, the timing of the devices is crucial. The raw data must be placed in the lab frame of time, and absolutely timed with the time of fusion as '0'. The timing of the scintillator was calculated with a series of x-ray shots, performed by using targets that, upon irradiation, predictably emit x rays over a short time period (<100 ps). Since x rays travel at a constant, known speed over the known distance, their expected time of arrival could be compared with the arbitrary time units ( $\tau$ ) recorded by the scintillator in order to develop absolute timing. In order to place the arbitrarily timed signal in a reference frame zeroed at the time of emission, the equation [3]:

$$t = \tau - (\tau_0 + \Delta t_{\text{laser}} + \Delta t_{\text{bang}}) - \Delta t_{\text{cal}} - \Delta t_{\text{att}}, \quad (2)$$

is used, where  $t$  is the true TOF of a signal;  $\tau$  is the arbitrary time units;  $\tau_0$  is the time of a measured fiducial (in this case the fiducial consists of a train of eight gaussian pulses) of the recorded signal;  $\Delta t_{\text{laser}}$  is the delay between the start of the laser pulse (defined as 2% of the maximum laser power) and the fiducial as reported by a P510 streak camera;  $\Delta t_{\text{bang}}$  is the delay between the neutron/x-ray bang time and the beginning of the laser pulse as reported by an NTD (neutron temporal diagnostic);  $\Delta t_{\text{cal}}$  is a calibration constant accounting for any inherent delays and mistiming in the detector device; and  $\Delta t_{\text{att}}$  accounts for additional delays in the signal timing if a signal attenuator is used.  $\Delta t_{\text{cal}}$  was calculated using x-ray shots, but was then applied to DD fusion shots as a timing constant.



The instrument response function (IRF) of the scintillator, photomultiplier tube, cables, and oscilloscope also plays an important role in the calibration of the nTOF diagnostics. It represents the measured signal generated by a single incident neutron on the complete detector system [4]. The IRF was calibrated with ten x-ray shots, and was found to be extremely stable. A typical IRF is shown in Figure 3.2, and resembles

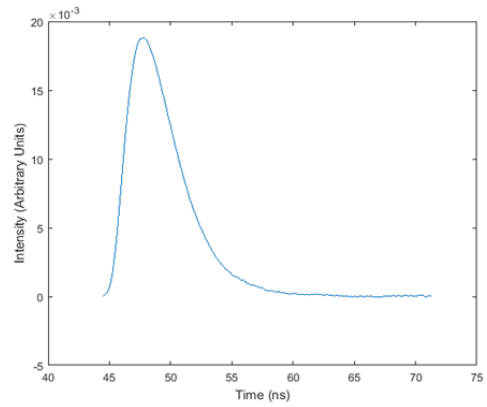


Figure 3.2  
Absolutely timed IRF curve from an x-ray shot. It is important to note that the pulse duration of the x-ray shot is much smaller than the timescale shown here.

an exponentially modified Gaussian. It is necessary to determine and account for this curve when fitting the raw data as it will influence the timing and shape of the data.

#### IV. FORWARD FIT METHOD

In order to fit the “raw” neutron time-of-flight data and determine the ion temperature and bulk flow velocity, a number of factors must be considered. The Matlab function “nlinfit” or “Nonlinear fit” allowed for the parametrization of  $dN/dE$  (the neutron energy distribution) so that the fitting procedure would independently determine values for the mean energy shift and ion temperature.

The standard form for the neutron energy distribution as determined by Ballabio [1] is as follows:

$$dN/dE = I_0 \exp\left(-\frac{2\bar{E}}{\sigma^2} (\sqrt{E} - \sqrt{\bar{E}})^2\right) \quad (2)$$

where

$$\bar{E} = \langle E \rangle \left[ 1 - \frac{3}{2} \left( \frac{\sigma_{\text{th}}}{\langle E \rangle} \right)^2 \right]^{\frac{1}{2}} \quad (3)$$

$$\sigma^2 = \frac{4}{3} \langle E \rangle^2 \left\{ \left[ 1 - \frac{3}{2} \left( \frac{\sigma_{\text{th}}}{\langle E \rangle} \right)^2 \right]^{\frac{1}{2}} - \left[ 1 - \frac{3}{2} \left( \frac{\sigma_{\text{th}}}{\langle E \rangle} \right)^2 \right] \right\} \quad (4)$$

$$= \frac{4}{3} \bar{E} [\langle E \rangle - \bar{E}] \quad (5)$$

$$E = E_0 + \Delta E_{\text{th}} \quad (6)$$

In Ballabio's semi-relativistic formula, the neutron distribution  $dN/dE$  (Equation 2) can be determined using  $I_0$ , a parameterized function of the standard deviation (ion temperature);  $\sigma^2$  as defined in Equations 4 and 5;  $E$  as defined in Equation 6; and  $\bar{E}$  as defined in Equation 3, representing the mean energy. Equations 3, 4 and 5 rely on  $\langle E \rangle$  and  $\sigma_{\text{th}}$ , which are parameterized functions of ion temperature (standard deviation). Equation 6 is in terms of  $E_0$ , representing the expected energy (2.45 MeV per neutron), and  $\Delta E_{\text{th}}$ , the expected energy shift as a function of ion temperature, yielding the expected mean energy without compensating for the mean energy shift from bulk flow velocity. To determine the value of the mean energy shift that is derived from a bulk flow velocity, the difference between  $\bar{E}$  and  $E$  is evaluated as a parametrized function of bulk flow velocity. Once the small shift in mean energy due to ion temperature is accounted

for, the remaining Doppler shifting of the mean velocity and, by extension, the neutron energy distribution, is dictated by the bulk flow velocity. By comparing the expected energy value of 2.45 MeV with the shifted energy value, a velocity shift can be derived by converting to the time-scale, and this velocity shift is indicative of the bulk flow velocity. [5]

The analysis discussed herein utilizes Ballabio’s formulas to determine  $dN/dE$  and derive values for mean energy shift and ion temperature. In order to match the “raw” data, the parameterized neutron energy distribution must be multiplied by the non-linear light output of the scintillator, and translated to the time/velocity scale of the data through the use of the relativistic energy equation, in which KE represents the energy of the neutrons,  $m_0$  represents neutron mass,  $c$  is the speed of light, and  $v$  is the velocity of the neutrons.

$$KE = m_0c^2 \left[ \frac{1}{\sqrt{1 - \frac{v^2}{c^2}}} - 1 \right] \quad (7)$$

Once the neutron distribution is translated to the time axis, it must be convolved with a neutron response and instrument response (as pictured in Figure 3.2) in order to accurately match the signal recorded by the oscilloscope. The neutron response function also accounts for the difference between the instrument response functions measured on x-ray shots and fusion shots [6].

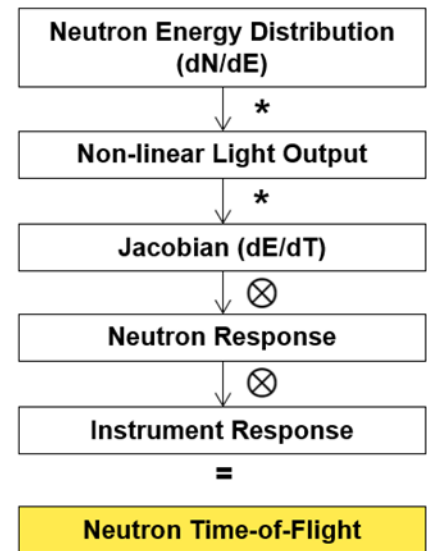


Figure 4.1  
Flow chart representing the inputs that contribute to the “raw” nTOF data.

A convolution is a mathematical function defined by the equation:

$$f(t) * g(t) \equiv \int_{-\infty}^{\infty} f(u)g(t-u)du \quad (8)$$

Convolutions function to incorporate characteristics of both input curves into a single output curve. This is especially useful when dealing with response functions as it allows for rapid application of response functions to complex inputs (i.e. the modified gaussian that serves to approximate the neutron energy distribution).

A step-by-step flowchart displaying how each of the functions contributes to the nTOF data that is being fit is presented in Figure 4.1, allowing for a better understanding of how this data is being reconstructed in terms of the desired parameters. The produced neutron time-of-flight curve  $I(t)$  is in terms of the parameters of ion temperature and mean energy shift, and therefore can be used as a fit function for MATLAB 's nonlinear fit tool. The nonlinear fit tool requires initial approximate test values for all parameters in order to more quickly and correctly fit the given function. Simulated predictions ( $\sim 3$  keV) were used as starting values for the fit. Once functional, the MATLAB code allowed for the rapid determination of ion temperature and mean energy shift from a neutron time of flight signal.

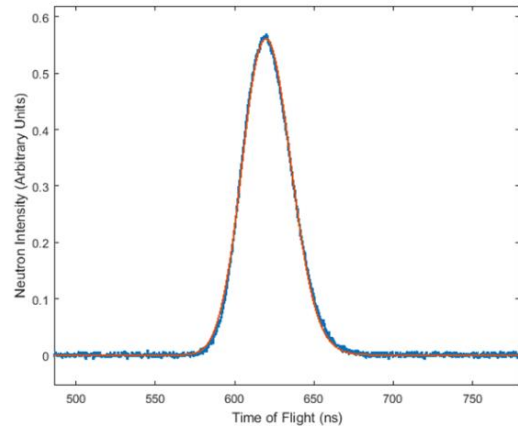


Figure 5.1  
The neutron time-of-flight signal data (blue) and parameterized fit from MATLAB (orange) on an induced-mode shot. The two curves are almost indistinguishable.

## V. APPLICATION OF ANALYSIS TO EXPERIMENTAL DATA

The fitting procedure described in Section IV was utilized to evaluate the ion temperature and bulk flow velocity of 35 nominal, well positioned shots and an induced-mode shot campaign investigating target offset. As seen in Figure 5.1, the signal and the parameterized fit for an induced-mode shot agree extremely well, indicating the quality of the fit.

Figure 5.2 shows the velocities obtained from 12 nominal shots. All analyzed shots yielded a strong positive bulk flow velocity, indicating an inherent asymmetry

### Sampled Bulk Flow Velocities

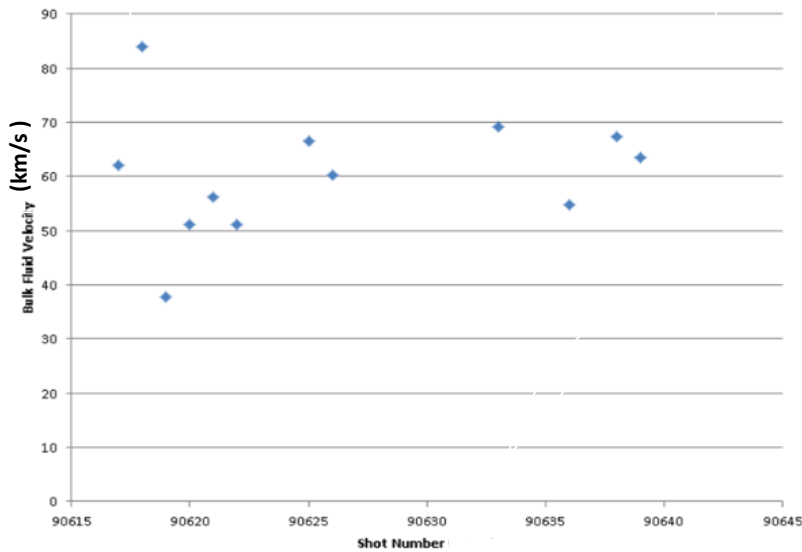


Figure 5.2  
A sample of bulk flow velocities plotted with respect to shot number. Nominal shots tended to have strong positive bulk flow velocities.

### Tion(shell thickness)

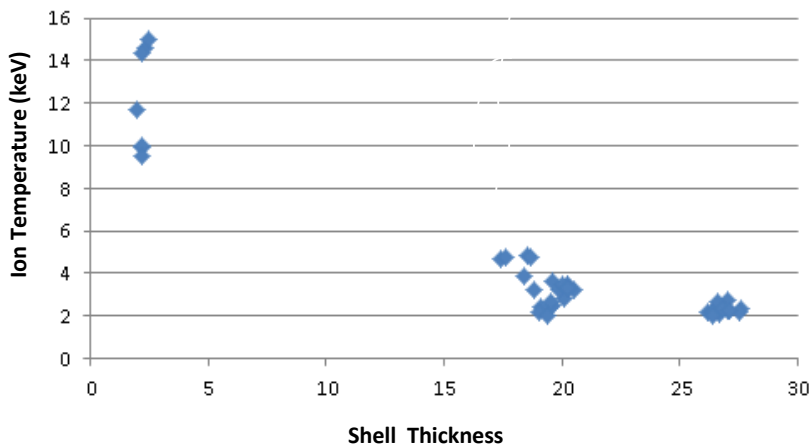


Figure 5.3  
Measured ion temperature as a function of shell thickness.

along the line of sight of the nTOF detector. It was also found that ion temperature was inversely related to shell thickness (Figure 5.3).

In addition to being applied to nominal shots, the analysis method was utilized to determine characteristics of plasmas in an induced-mode campaign in which intentional target offsets were applied. Since these shots were performed long before the timeframe of the research described herein, radiation hydrodynamic simulations such as Figure 5.4 for a 40-um offset had already been developed for the series of shots, and expected values for the bulk flow velocity had been determined. The experimental data from these shots was analyzed, and the agreement between the expected and experimental values was close (Figure 5.5). Just as the nominal shots had all yielded a positive bulk flow velocity, most of the experimentally determined velocities consistently overshoot the simulated values by amounts that ranged from 10 km/s to 45 km/s (Figure 5.5).

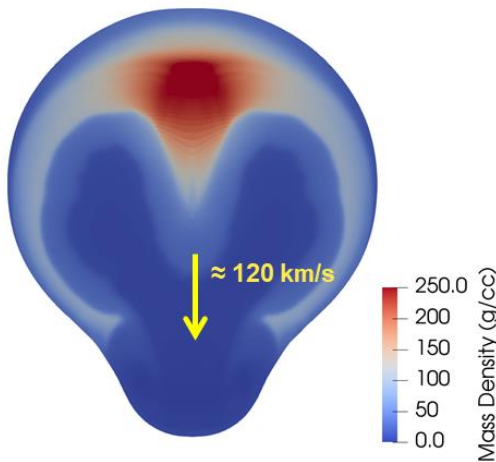


Figure 5.4  
DRACO simulation of plasma density on a target with a 40 micron offset in the positive y-direction. [7]

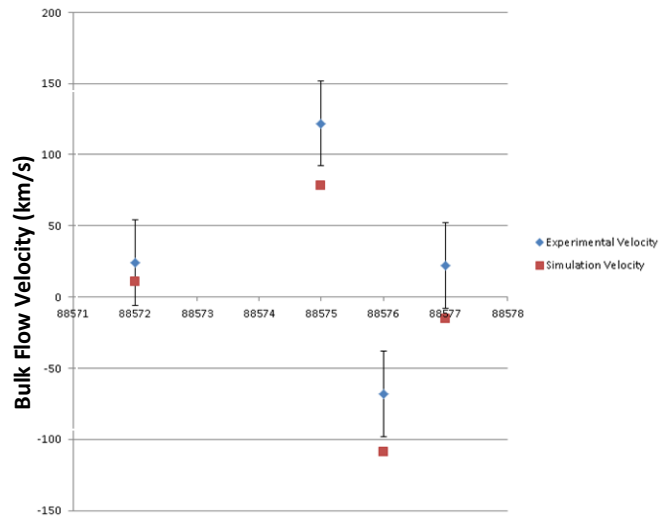


Figure 5.5  
Experimental and simulated values for bulk flow velocity for four shots with various target offsets. Agreement is clear, but a consistent positive shift of experimental values indicates a systematic imbalance.

Experimental induced-mode shots could provide data with which to correct the inherent asymmetry in the system suggested by Figures 5.2 and 5.5. As seen in Figure 5.6, which plots data from the same four shots as a function of target offset, bulk flow velocity is directly related to the target offset. The average bulk flow velocity found on 0-offset control shots of the target-offset campaign is approximately 30 km/s as seen

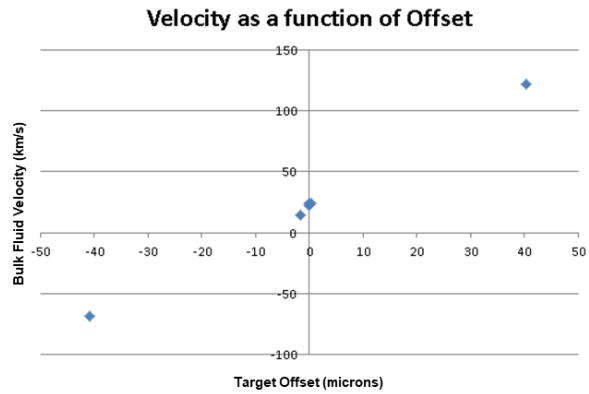


Figure 5.6 Bulk flow velocity as a function of target offset for the four shots plotted in figure 5.5. A direct linear relationship between target offset and bulk flow velocity is clearly visible even with minimal data.

in Figure 5.6, which is less than the bulk flow velocity found on 0-offset nominal shots. More data is therefore required to accurately determine the bulk flow velocity produced by a 0-offset shot. By performing more experimental shots and gathering more data, a linear trend line can be approximated for a plot similar to Figure 5.6, with the x-intercept yielding a target offset that would counteract the inherent asymmetry of the system.

## VI. CONCLUSION

A forward-fit analysis technique was developed to evaluate the ion temperature and bulk flow velocity of a primary (DD) neutron energy distribution from a neutron time-of-flight spectrometer. This approach was utilized in a recent campaign to measure the effect of intentional target offset. Through comparison with existing data and simulations, the technique was found to be relatively accurate in determining ion temperatures and bulk flow velocities, the latter indicating an inherent asymmetry in the

laser-target system. In the future, more data from target-offset shots could potentially provide enough information to design a standardized offset to eliminate the inherent asymmetry.

## VII. ACKNOWLEDGEMENTS

I would like to thank Chad Forrest, my project advisor who so patiently and expertly taught me everything I needed to know. I would like to thank Owen Mannion who kindly helped debug my code on multiple occasions and served as a resource for when I was stuck. I would like to thank the other participants in the High School program, for providing much-needed moral support and always being willing to offer a fresh set of eyes or a new mathematical trick. Finally, I would like to thank Dr. Stephen Craxton, who made the High School Research Program what it is today, and so patiently aided in the editing and revision of this report.

## References

1. L. Ballabio, J. Källne, and G. Gorini, Nucl. Fusion **38**, 1723 (1998).
2. D. H. Munro et al., Phys. Plasmas **24**, 056301 (2017).
3. O.M. Mannion, Review of Scientific Instruments **89** 10I131 (2018).
4. X. Y. Peng, Review of Scientific Instruments **87**, 11D836 (2016).
5. B. Appelbe and J. Chittenden, Plasma Phys. Control. Fusion **53**, 045002 (2011).
6. R. Hatarik, Journal of Applied Physics **118**, 184502 (2015).
7. D. Keller, T. J. B. Collins, J. A. Delettrez, P. W. McKenty, P. B. Radha, B. Whitney, and G. A. Moses, Bull. Am. Phys. Soc. **44**, 37 (1999)